

# Effect of synthesized temperature on microstructure, infrared emissivity and dielectric property of Fe-doped ZnO powder

Xiaolei Su · Xiaoqin Liu · Yan Jia ·  
Junbo Wang · Jie Xu · Xinhai He · Chong Fu ·  
Songtao Liu · Jing Zheng

Received: 22 July 2013 / Accepted: 26 September 2013 / Published online: 4 October 2013  
© Springer Science+Business Media New York 2013

**Abstract** Fe-doped ZnO powder has been synthesized by coprecipitation method under different synthesized temperature, using zinc nitrate as the starting material, urea as the precipitator, and ferric nitrate as the doping source, respectively. The prepared powders have been characterized by XRD and SEM. Results show that when the synthesized temperature is below 700 °C the prepared powders are ZnO(Fe) solid solution powders and the ZnFe<sub>2</sub>O<sub>4</sub> impurity phase appeared for the Fe-doped ZnO powder synthesized at 700 °C. The electric permittivities in the frequency range of 8.2–12.4 GHz and average infrared emissivity at the waveband range of 8–14 μm of prepared powders have been determined. The real part and imaginary part of electric permittivities of prepared powders have increased firstly and then decreased with increasing synthesized temperature. The average infrared emissivity has presented the opposite changing trend.

## 1 Introduction

ZnO, a direct wide band gap (3.37 eV) semiconductor, has many excellent properties, for example, nontoxic, cheap, unique optical and electrical properties, which has wide applications in the nanolasers, piezoelectric nanogenerators, solar cells, gas sensors, photocatalyst, and so on [1–3].

In recent years, increasing levels of electromagnetic pollution (due to the use of electronic and telecommunication systems) have recently focused attention on the absorbing material, especially ZnO materials, in the microwave range [4].

Chen et al. [4] have fabricated the tetrapod-like ZnO nanostructures by rapid heating metal zinc pellet at 900 °C under air ambient. The ZnO nanowire-polyester composites, which fabricated into a planar plate with the area 180 mm × 180 mm and the thickness of about 1 mm, show the good microwave absorption in the frequency range of 2–18 GHz. Cao and Zhou et al. [5, 6] have prepared ZnO nanowire-polyester composites and composite coatings containing ZnO whisker, respectively, and show the strong microwave absorption in X band. Kong et al. [7] have prepared Al-doped ZnO/ZrSiO<sub>4</sub> composite ceramics and studied the dielectric loss and microwave absorption properties in the frequency range of 8.2–12.4 GHz. According to the calculation of reflection loss by the  $\epsilon'$  and  $\epsilon''$  values, the maximum reflection loss reaches –32 dB at 9.2 GHz with a thickness of 3.5 mm. Yuan Wang et al. [8] have synthesized Al-doped ZnO (AZO) powders with different Al concentrations were synthesized by a coprecipitation method. The  $\epsilon'$  and  $\epsilon''$  of prepared AZO has been improved in the frequency range of 8.2–12.4 GHz due to the Al<sub>Zn</sub> defects generated by the substitution of Zn ions by Al ions. Zhuo et al. [9] have synthesized intriguing ZnO dendritic nanostructures by a two-step chemical vapor deposition process. The value of maximum reflection loss for the composite with 50 vol.% ZnO dendritic nanostructures reached –42 dB at 3.6 GHz with a thickness of 5.0 mm. Tang et al. [10] have prepared Fe-doped ZnO coated barium ferrite composite particles by a heterogeneous precipitation and thermal treatment process. The absorbing property has been improved and adjusted by

X. Su (✉) · X. Liu · Y. Jia · J. Wang · J. Xu · X. He ·  
C. Fu · S. Liu  
College of Mechanical and Electronic Engineering, Xian  
Polytechnic University, Xi'an 710048, Shaanxi, China  
e-mail: suxlei@163.com

J. Zheng  
Electronic Materials Research Center, Northwest Institute for  
Nonferrous Metal Research, Xi'an 710016, Shaanxi, China

changing the thickness of ZnO coverage in the frequency range of 2–12 GHz. It can be seen that the Fe-doped ZnO shows the good microwave absorption property.

Meanwhile, ZnO has also showed good infrared emissivity at the waveband range of 8–14  $\mu\text{m}$  according to related research. Yao et al. [11] have synthesized  $\text{Zn}_{0.99-x}\text{Mn}_{0.01}\text{Co}_x\text{O}$  ( $x = 0.00, 0.01, 0.03, 0.05$ ) powders at different calcination temperatures by a solid-state reaction and the minimum infrared emissivity value reach 0.754. Shuyuan Zhang et al. [12] have synthesized the Co-doped ZnO powders by the conventional solid state reaction, and presented the infrared emissivity at the waveband range of 3–5  $\mu\text{m}$  and 8–14  $\mu\text{m}$  and microwave absorption property in the frequency range of 8.2–12.4 GHz. It can be seen that the prepared Co-doped ZnO powder has both good microwave absorption property and good infrared emissivity. Therefore, because the Fe element belongs to the VIII group, it presents the same effect on SiC powder as the Co element possibly.

Therefore, Fe-doped ZnO powder may achieve the composite stealth in the X band frequency and 8–14  $\mu\text{m}$  waveband. In the paper, Fe-doped ZnO powders were synthesized by coprecipitation method under different reaction temperature, using zinc nitrate as the starting material, urea as the precipitator and ferric nitrate as the doping source, respectively. The dielectric property in the frequency range of 8.2–12.4 GHz and average infrared emissivity at the waveband range of 8–14  $\mu\text{m}$  have been determined. The effects and mechanism of reaction temperature on microstructure, dielectric property and infrared emissivity of ZnO(Fe) powders have been discussed.

## 2 Experimental

### 2.1 Sample preparation

Fe-doped ZnO powders were synthesized by coprecipitation method, using zinc nitrate ( $\text{Zn}(\text{NO}_3)_2 \cdot 6\text{H}_2\text{O}$ ) as the starting material, urea ( $\text{CO}(\text{NH}_2)_2$ ) as the precipitator and ferric nitrate ( $\text{Fe}(\text{NO}_3)_3 \cdot 9\text{H}_2\text{O}$ ) as the doping source, respectively. All the chemical reagents were analytical grades and used without further purification.

Firstly,  $\text{Zn}(\text{NO}_3)_2 \cdot 6\text{H}_2\text{O}$ ,  $\text{Fe}(\text{NO}_3)_3 \cdot 9\text{H}_2\text{O}$  and  $\text{CO}(\text{NH}_2)_2$  were separately dissolved in de-ionized water. Secondly, appropriate amounts of  $\text{Fe}(\text{NO}_3)_3 \cdot 9\text{H}_2\text{O}$  solutions were added into the  $\text{Zn}(\text{NO}_3)_2 \cdot 6\text{H}_2\text{O}$  solution according to the experimental design. In our study, the molar ratio of Fe to (Zn + Fe),  $n_{\text{Fe}}/(n_{\text{Fe}}+n_{\text{Zn}})$ , is 0.06. Finally,  $\text{CO}(\text{NH}_2)_2$  solution was slowly added into these above mixture solutions. The as-prepared solutions were continually stirred at 100 °C for 1 h to yield precipitates. After filtered, the

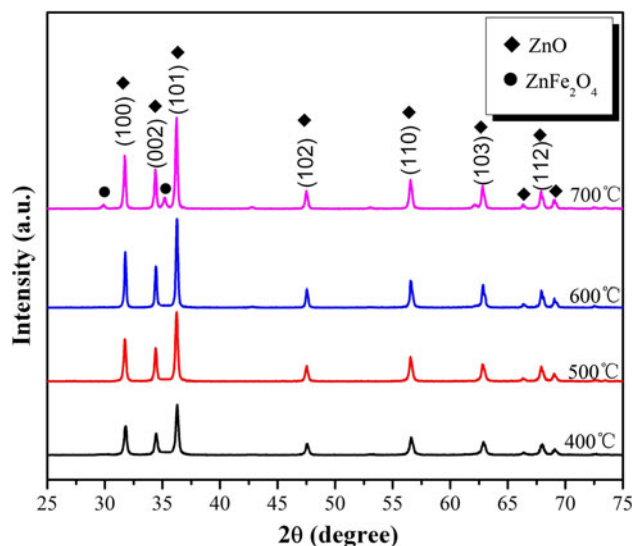


**Fig. 1** XRD patterns of the prepared Fe-doped ZnO powders at different synthesized temperature

precipitates were washed with distilled water and ethanol several times, dried in air at 120 °C in stove. Fe-doped ZnO powders were obtained after the precipitates were annealed at 400, 500, 600 and 700 °C, respectively, for 1 h.

### 2.2 Microstructure, infrared emissivity and dielectric property characterization

The products were identified by X-ray diffraction (XRD, X'Pert PRO MPD, Cu  $K\alpha$ ) to detect the generated phases. The 99.99 % Si ( $a = 5.43088 \text{ \AA}$ ) was used as inner standard. The morphology of the prepared powders was investigated by scanning electron microscope (SEM, JSM-6360LV, JEOL, Tokyo, Japan). The mean infrared emissivity at the waveband range of 8–14  $\mu\text{m}$  was measured by the reference method [12]. Because of the low dielectric loss of paraffin, the samples for dielectric parameters measurement at room temperature were prepared by mixing the produced powders with paraffin in a mass ratio of 10:90, and then the mixtures were molded into a brass flange to fabricate rectangular composite samples with the dimensions of 10.16 mm (width)  $\times$  22.86 mm (length)  $\times$  2 mm (thickness). The dielectric parameters were carried out by waveguide technique with mode TE<sub>10</sub> in the frequency range of 8.2–12.4 GHz, with the prepared samples set in a brass holder in which fills the waveguide. After being calibrated with an intermediate of a short circuit and blank holder, reflection and transmission losses were obtained by PNA network analyzer (Agilent Technologies E8362B, Palo Alto, CA), and then both the real and imaginary parts of the permittivity were given.

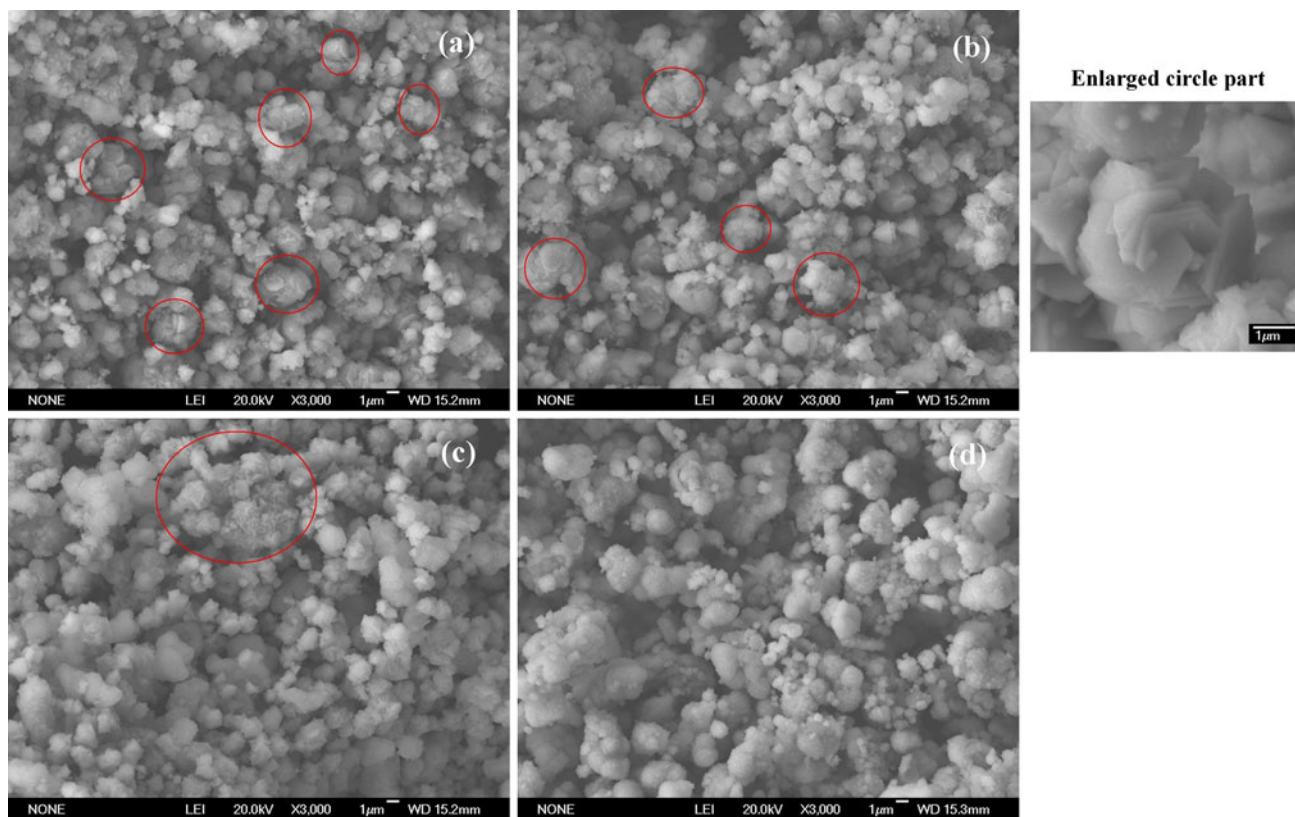


**Fig. 2** SEM images of the prepared Fe-doped ZnO powders at different synthesized temperature; **a** 400 °C; **b** 500 °C; **c** 600 °C and **d** 700 °C

### 3 Results

#### 3.1 XRD patterns

Figure 1 shows XRD patterns of the prepared Fe-doped ZnO powders at different synthesized temperature. It can be seen that all appearing peaks at  $2\theta = 31.78^\circ, 34.38^\circ, 36.28^\circ, 47.70^\circ, 56.66^\circ, 62.86^\circ, 68.00^\circ$  for all samples synthesized at 400, 500 and 600 °C belong to the ZnO phase and no the other impurities phase corresponding to Fe compounds have been observed in the XRD patterns. However, for the sample synthesized at 700 °C the  $\text{ZnFe}_2\text{O}_4$  impurity phase has been observed besides ZnO phase.

#### 3.2 SEM images

Figure 2 shows the SEM images of the prepared Fe-doped ZnO powders at different synthesized temperature. It can be seen that all prepared powders have presented the narrow size distribution and the size of powder shows a little increase with increasing synthesized temperature. The reason is that the higher reaction temperature improves the crystal growth of ZnO. In addition, amounts of flowerlike ZnO powders, as shown in enlarged circle part of Fig. 2, decreased with increasing synthesized temperature.

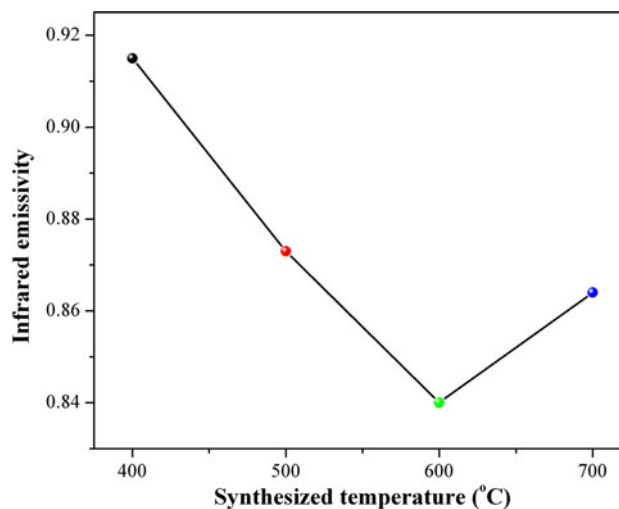


**Fig. 3** Infrared emissivity of prepared Fe-doped ZnO powder as a function of synthesized temperature

#### 3.3 Infrared emissivity

Figure 3 shows the infrared emissivity of prepared ZnO powder as a function of synthesized temperature. It can be seen that the infrared emissivities of prepared Fe-doped ZnO powder at 400, 500, 600 and 700 °C, which are 0.915,

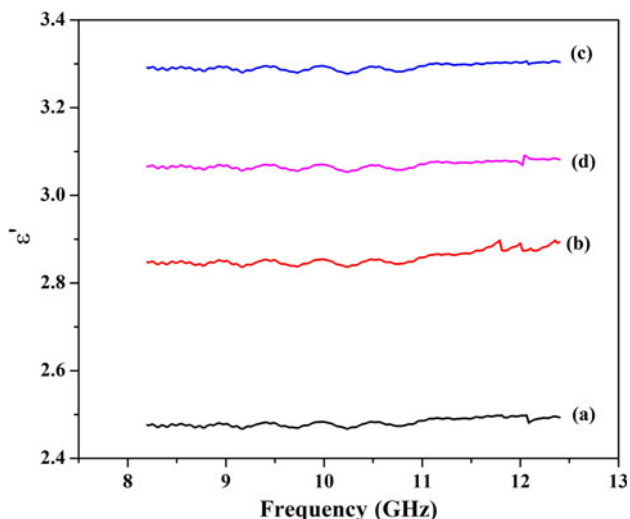


**Fig. 4** Real part  $\epsilon'$  of complex permittivity as a function of frequency in the frequency range of 8.2–12.4 GHz for the prepared Fe-doped ZnO powders at different synthesized temperature; *a* 400 °C; *b* 500 °C; *c* 600 °C and *d* 700 °C

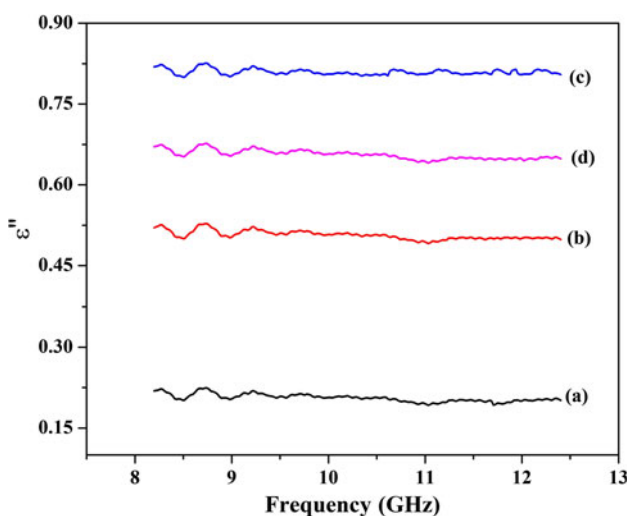


**Fig. 5** Imaginary part  $\epsilon''$  of complex permittivity as a function of frequency in the frequency range of 8.2–12.4 GHz for the prepared Fe-doped ZnO powders at different synthesized temperature; *a* 400 °C; *b* 500 °C; *c* 600 °C and *d* 700 °C

0.873, 0.84 and 0.864, respectively, decrease firstly and then increase with increasing synthesized temperature.

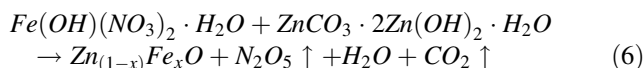
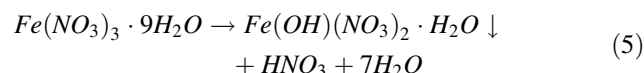
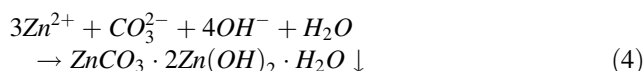
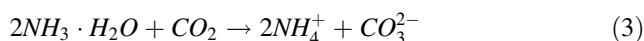
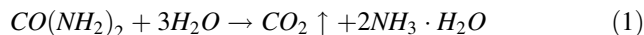
### 3.4 Dielectric property

Figures 4 and 5 show the real part  $\epsilon'$  and imaginary part  $\epsilon''$  of complex permittivity as a function of frequency for the prepared Fe-doped ZnO powders at different synthesized temperature. It can be seen that the  $\epsilon'$  and  $\epsilon''$  of the prepared Fe-doped ZnO powders at 400, 500, 600 and 700 °C are about 2.48 and 0.17, 2.86 and 0.52, 3.3 and 0.83, and 3.07

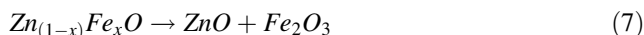
and 0.68, respectively. It shows that the dielectric properties of prepared powders increased firstly and then decreased with increasing synthesized temperature.

## 4 Discussions

When the synthesized temperature is below 700 °C, the SiC(Fe) solid solution powders have been prepared successfully by the reactions (1) to (6):



For the generation of ZnFe<sub>2</sub>O<sub>4</sub> impurity phase at 700 °C in XRD patterns, the reason is possible that the excess synthesized temperature leads to the precipitation of Fe from ZnO crystal and generation ZnFe<sub>2</sub>O<sub>4</sub> impurity phase by the reactions (7) and (8).



The lattice constants *a* and *c* of all samples have been calculated by Bragg formula and are *a* = 3.24753, 3.24287, 3.24024 and 3.2406 Å, and *c* = 5.20660, 5.20273, 5.17431 and 5.20242 Å, respectively, as shown in Figs. 6 and 7. It can be seen that lattice constant *a* decrease firstly and then increase with increasing synthesized temperature and lattice constant *c* presents the same changing trend. The reason is possible that during the synthesized process of ZnO powders the Fe atoms have entered the ZnO lattice, have substituted Zn atoms preferentially and have generated Fe<sub>Zn</sub> defects. Because of the ion radius of Fe<sup>3+</sup> (0.645 Å) smaller than that of Zn<sup>2+</sup> (0.74 Å) the decrease of lattice constant is caused by the substitution of Zn atoms of ZnO lattice by the Fe atoms, which leads to the decrease of lattice constant *a* and *c* of Fe-doped ZnO. The lattice constants have decreased with increasing synthesized temperature due to the more Fe atoms entering ZnO crystal, the more substitutions of Zn ions by Fe ions and the more generated Fe<sub>Zn</sub> defects. However, because Fe atoms have precipitated from Fe-doped ZnO crystal synthesized at 700 °C, the ZnFe<sub>2</sub>O<sub>4</sub> impurity phase has been generated, which leads to the decrease of Fe<sub>Zn</sub> defects amounts. So, the

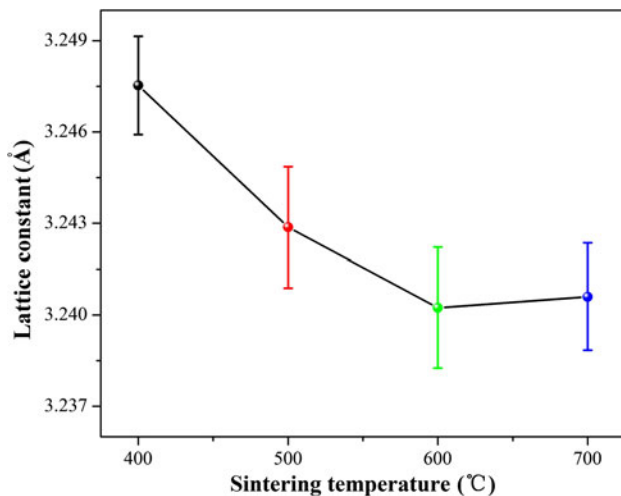


**Fig. 6** Lattice constant *a* of prepared ZnO powder as a function of synthesized temperature

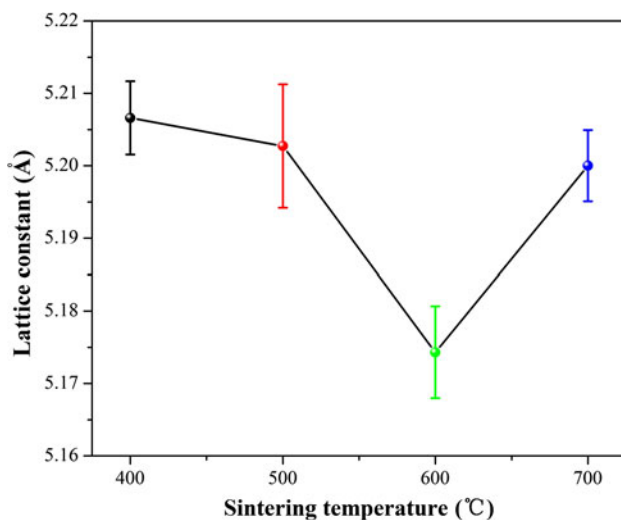


**Fig. 7** Lattice constant *c* of prepared ZnO powder as a function of synthesized temperature

lattice constant of Fe-doped ZnO has presented a little increase.

For the decrease of flowerlike ZnO powder, the related study indicates that the formation of ZnO includes nucleation and crystal growth [13]. Because the nucleation rate is relatively high, a large amount of ZnO nuclei has been generated and the ZnO crystal grows slowly. A quantity of ZnO nuclei or generated tiny single crystals aggregate together under the driving forces of surface energy, electrostatic force, and so on, at the early stage. And then, the each aggregated ZnO nucleus grows anisotropically along its *c*-axis. So the obtained structure is comprised of several single crystals aggregated along certain directions, which improves the formation of flower like ZnO powders. However, because Fe-doping will disturb the crystal

growth of ZnO and reduce the amounts of aggregated ZnO nucleus growing anisotropically along *c*-axis, the more amounts of Fe atoms entering ZnO lattice leads to decreasing amounts of flowerlike ZnO powder. The flowerlike ZnO powder synthesized at 700 °C almost disappeared due to the precipitation of Fe from ZnO crystal and generation of ZnFe<sub>2</sub>O<sub>4</sub> impurity phase possibly.

According to the analysis of XRD, when Fe atoms entered ZnO lattice the substitution of Zn atoms by Fe atoms and the Fe<sub>Zn</sub> defects have been generated. Because the Fe atoms present trivalent state usually and have three electrons bonded with the other element, amounts of bound electrons exist around Fe<sub>Zn</sub> defects in the ZnO crystal. At the same time, because the Fe-doped ZnO is an ionic crystal and relative vibration between different ions will produce a certain change in the electric dipole moment, which will produce the interaction between long optical wave and infrared radiation and then infrared radiation is generated and absorbed. So, the more Fe<sub>Zn</sub> defects have been generated, the more infrared radiation has been produced. According to analysis of XRD, because the Fe atom concentration entering ZnO lattice increased firstly and then decreased with increasing synthesized temperature, the Fe<sub>Zn</sub> defect concentration presented the same changing trend. Because the interaction of Fe<sub>Zn</sub> defect and infrared radiation influences the change of infrared emissivity of prepared Fe-doped ZnO powders, the infrared emissivity shows the same changing trend as the Fe atom concentration entering ZnO lattice with increasing synthesized temperature. Therefore, the Fe-doped ZnO powder synthesized at 600 °C presented the lowest infrared emissivity at the waveband range of 8–14 μm.

When the Fe atoms entered the ZnO lattice, the substitutions of Zn atoms by Fe atoms have been generated. There is a mounts of bound electrons around Zn<sub>Fe</sub> defects in the ZnO crystal. Under the alternating electromagnetic field, these bound electrons will migrate to and fro to form relaxation polarization and loss, thus leading to the higher ε' and ε'', respectively. Because the higher ε'' suggests a better capacity of dielectric loss in the microwave range, the prepared Fe-doped ZnO powder at 600 °C has the best microwave absorption in the frequency range of 8.2–12.4 GHz.

## 5 Conclusions

Fe-doped ZnO powder has been produced successfully by coprecipitation method at 400, 500, 600 and 700 °C, using zinc nitrate as the starting material, urea as the precipitator, and ferric nitrate as the doping source, respectively. When the synthesized temperature is below 700 °C the prepared powder is ZnO(Fe) solid solution powders and the

ZnFe<sub>2</sub>O<sub>4</sub> impurity phase appeared for the Fe-doped ZnO powder synthesized at 700 °C due to the precipitation of Fe from ZnO crystal. The amount of flowerlike ZnO powder decreased with increasing synthesized temperature due to the Fe-doping. The average infrared emissivity at the waveband range of 8–14 μm of prepared Fe-doped ZnO powders decreased firstly and then increased and the  $\epsilon'$  and  $\epsilon''$  in the frequency range of 8.2–12.4 GHz presented the opposite trend with increasing synthesized temperature due to the generated Fe<sub>Zn</sub> defects concentration. The prepared Fe-doped ZnO powder at 600 °C achieves the composite stealth in the X band and 8–14 μm waveband possibly.

**Acknowledgments** The authors gratefully acknowledge the support of the National Natural Scientific Foundation of China (Grant No. 51002113), the Natural Science Basic Research Plan in Shaanxi Province of China (Grant No. 2012JQ6021 and No. 2013JM6008) and Foundation of Shaanxi Educational Committee (Grant No. 2013JK0932).

## References

1. Z.L. Wang, MRS Bull. **37**, 2012 (814)
2. M.H. Huang, S. Mao, H. Feick, H. Yan, W. Yiyang, H. Kind, E. Weber, R. Russo, P. Yang, Science **292**, 1897 (2001)
3. Z.L. Wang, Mater. Sci. Eng. R **64**, 33(2009)
4. Y.J. Chen, M.S. Cao, T.H. Wang, Q. Wan, Appl. Phys. Lett. **84**, 3367 (2004)
5. M.-S. Cao, X.-L. Shi, X.-Y. Fang, H.-B. Jin, Z.-L. Hou, W. Zhou, Y.-J. Chen, Appl. Phys. Lett. **91**, 203110 (2007)
6. Z.W. Zhou, S.K. Liu, L.X. Gu, J. Appl. Polym. Sci. **80**, 1520 (2001)
7. L. Kong, X. Yin, L. Zhang, L. Cheng, J. Am. Ceram. Soc. **95**, 3158 (2012)
8. Y. Wang, F. Luo, L. Zhang, D. Zhu, W. Zhou, Ceram. Inter. (2013). doi:10.1016/j.ceramint.2013.04.056
9. R.F. Zhuo, H.T. Feng, J.T. Chen, D. Yan, J.J. Feng, H.J. Li, B.S. Geng, S. Cheng, X.Y. Xu, P.X. Yan, J. Phys. Chem. C **112**, 11767 (2008)
10. X. Tang, H. Ke-Ao, Mater. Sci. Eng. B **139**, 119 (2007)
11. Y. Yin-Hua, C. Quan-Xi, Chin. Phys. B **21**(12), 124205 (2012)
12. Z. Shuyuan, C. Quanxi, Adv. Mater. Res. **399–401**, 880 (2012)
13. P. Li, H. Liu, Y.-F. Zhang, Y. Wei, X.-K. Wang, Mater. Chem. Phys. **106**, 63 (2007)